International Journal of Antimicrobial Agents 66 (2025) 107587

Contents lists available at ScienceDirect

International Journal of Antimicrobial Agents

journal homepage: www.elsevier.com/locate/ijantimicag

Prediction of methicillin-resistant *Staphylococcus aureus* and carbapenem-resistant *Klebsiella pneumoniae* from Raman spectra by Artificial Intelligent Raman Detection and Identification System (AIRDIS) with machine learning

Hsiu-Hsien Lin[a,†], Yu-Tzu Lin[b,†], Chih-Hao Chen[c], Kun-Hao Tseng[a], Pang-Chien Hsu[a], Ya-Lun Wu[d], Wei-Cheng Chang[e], Nai-Shun Liao[e], Yi-Fan Chou[e], Chun-Yi Hsu[e], Yu-Hui Liao[e], Mao-Wang Ho[c], Shih-Sheng Chang[d], Po-Ren Hsueh[a,c,*], Der-Yang Cho[f]

[a] *Department of Laboratory Medicine, China Medical University Hospital, China Medical University, Taichung City, Taiwan*
[b] *Department of Medical Laboratory Science and Biotechnology, China Medical University, Taichung City, Taiwan*
[c] *Department of Internal Medicine, Division of Infectious Diseases, China Medical University Hospital, China Medical University, Taichung City, Taiwan*
[d] *AI Innovation Center, China Medical University Hospital, Taichung City, Taiwan*
[e] *ITRUST MedTech Inc., Hsinchu, Taiwan*
[f] *Department of Neurosurgery, China Medical University Hospital, Taichung City, Taiwan*

ARTICLE INFO

Article history:
Received 28 January 2025
Accepted 19 July 2025

Editor: Professor Jian Li

Keywords:
Artificial Intelligence
Machine learning
Raman spectra
Prediction
Methicillin-resistant *Staphylococcus aureus*
Carbapenem-resistant *Klebsiella pneumoniae*

ABSTRACT

Objectives: Methicillin-resistant *Staphylococcus aureus* (MRSA) and carbapenem-resistant *Klebsiella pneumoniae* (CRKP) are two of the most important antibiotic-resistant bacteria. Early use of the correct treatment strategy can not only reduce patient mortality but also prevent the development of resistance. Although some rapid but costly techniques are available, routine workflows in clinical microbiology laboratories can sometimes take several days to deliver bacterial identification and resistance profiles. In this study, we developed a bacterial identification and resistance prediction system that combines Raman spectroscopy and machine learning to predict the MRSA and CRKP.

Methods: A total of 988 *S. aureus* isolates (including 513 MRSA) and 1053 *K. pneumoniae* isolates (including 517 CRKP) were collected. Of these, 266 *S. aureus* isolates and 285 *K. pneumoniae* isolates were used for training, while the remainder were used for validation.

Results: The system demonstrated high predictive performance, with accuracy and area under receiver operating characteristic (AUROC) values of 88% and 0.92 for MRSA prediction and 87% and 0.96 for CRKP prediction, respectively.

Conclusions: As a result, we confirmed the ability of machine learning to interpret Raman spectra for predicting resistant bacteria in clinical microbiology laboratories. This is the first and novel system validated with a large number of clinical isolates and may be incorporated into existing workflows.

1. Introduction

Antimicrobial resistance (AMR) poses an urgent global health threat. The World Health Organization's 2024 bacterial priority pathogens list highlights that antibiotic-resistant bacteria, including *Staphylococcus aureus* and *Klebsiella pneumoniae*, were responsible for 1.27 million deaths in 2019, with a total of 5 million deaths associated with AMR worldwide [1]. In routine workflows, antimicrobial susceptibility testing is usually performed after bacterial identification and relies on culture-based methods [2]. Before definitive results is available, clinicians rely on empirical antibiotic therapy, often using broad-spectrum antibiotics. This approach not only exacerbates the problem of antimicrobial resistance but also increases the risk of adverse effects on patients [3].

Current routine methods used in clinical microbiology laboratories, such as AST, matrix-assisted laser desorption/ionization time-of-flight mass spectrometry (MALDI-TOF MS), and molecular detection of resistance genes, are essential but have limitations.

* Corresponding author. Mailing address: Department of Laboratory Medicine, China Medical University Hospital, China Medical University, No. 2, Yude Road, North District, Taichung City 40447, Taiwan
E-mail addresses: hsporen@gmail.com, hsporen@ntu.edu.tw (P.-R. Hsueh).
† These authors contributed equally to this study.

https://doi.org/10.1016/j.ijantimicag.2025.107587

AST provides reliable susceptibility profiles but is time-consuming. MALDI-TOF MS offers rapid and cost-effective species identification, and recent studies have explored its potential for AMR prediction using machine learning; however, such applications are not yet widely implemented in routine clinical workflows. Therefore, a rapid method capable of predicting antimicrobial resistance phenotypes with clinical applicability would be of great value.

Raman spectroscopy uses monochromatic light to exploit inelastic scattering, known as the Raman effect. This phenomenon occurs when photons are excited to virtual energy states, resulting in either a loss (Stokes) or gain (anti-Stokes) of energy due to interactions with the vibrational modes of chemical bonds within the sample. These energy shifts correspond to discrete vibrational modes of polarizable molecules, enabling qualitative analysis of the biochemical composition. Although inelastic scattering is relatively inefficient, Raman spectroscopy can still provide valuable chemical bond information, even in hydrated environments [4]. Moreover, quantitative data can be obtained if the instrument response function is appropriately corrected [4–6].

Raman spectroscopy, as a non-destructive, rapid, and highly sensitive analytical method, has demonstrated significant potential in the biomedical field. Bacteria with different phenotypes are composed of unique molecules, resulting in subtle variations in their Raman spectra [7]. This attribute confers high specificity to the Raman signal [8]. Additionally, due to its non-invasive and label-free nature, Raman spectroscopy has demonstrated potential in the identification of microbial species and the detection of antibiotic resistance [8]. However, the complexity and high dimensionality of Raman spectral data present significant challenges for data analysis.

Deep learning techniques, particularly convolutional neural networks (CNN), offer significant advantages in handling high-dimensional data and image recognition tasks [9]. Applying deep learning to the analysis of Raman spectral data enables automatic feature extraction and classification, thereby enhancing the accuracy and efficiency of antimicrobial resistance prediction. Preliminary studies have demonstrated the potential of combining Raman spectroscopy with machine learning to predict resistant strains [10–13]. However, its direct application in clinical microbiology laboratories still requires further validation.

This study aims to develop the Artificial Intelligent Raman Detection and Identification System (AIRDIS), which utilizes Raman spectroscopy combined with deep learning techniques to predict methicillin-resistant *S. aureus* (MRSA) and carbapenem-resistant *K. pneumoniae* (CRKP) – two antibiotic-resistant strains that present significant challenges in clinical treatment. By establishing and training deep learning models, we aim to achieve rapid and accurate identification of resistant strains, providing strong support for clinical diagnosis and treatment.

This device, the Artificial Intelligent Raman Detection and Identification System (AIRDIS, C240069), does not meet the requirements of current regulations and has been recommended for classification under the De Novo pathway by the U.S. Food and Drug Administration (FDA) on October 15, 2024.

2. Material and methods

2.1. Study workflow

In this study, the identification of MRSA and CRKP from clinical specimens was based on a routine laboratory workflow, which included species identification using the matrix-assisted laser desorption/ionization time-of-flight mass spectrometry (MALDI-TOF MS) MALDI-TOF MS Biotyper system (Bruker Microflex LT/SH, Bruker Daltonics GmbH, Bremen, Germany) and antimicrobial susceptibility testing performed with the automated Phoenix system (Phoenix M50, Becton–Dickinson Microbiology Systems, Sparks, MD, USA).

Table 1
Bacteria isolates evaluated in this study.

Organism	No. of isolates collected	
	CMUH	SMART
S. aureus	362	626
MRSA	211	302
MSSA	151	324
K. pneumoniae	447	606
CRKP	217	300
CSKP	230	306

MRSA, methicillin-resistant *S. aureus;* MSSA, methicillin-susceptible *S. aureus;* CRKP, carbapenem-resistant *K. pneumoniae;* CSKP, carbapenem-susceptible *K. pneumoniae*; CMUH, China Medical University Hospital; SMART, Surveillance of Multicentre Antimicrobial Resistance in Taiwan.

To explore the feasibility of applying Raman spectroscopy combined with deep learning for clinical bacterial identification and antimicrobial resistance prediction, bacterial spectral data were collected using a Raman spectrometer. The species identification results from the MALDI-TOF MS Biotyper system, along with the antimicrobial susceptibility test results from the automated Phoenix system, were used as labels for the bacterial Raman spectra, facilitating deep learning modelling and validation. This model was designed to be compatible with existing clinical workflows, potentially allowing simultaneous bacterial identification and antimicrobial resistance prediction without requiring additional experimental equipment, as shown in Fig. 1.

2.2. Bacterial isolates

A total of 2041 clinical isolates were collected from two sources, comprising 988 *S. aureus* isolates (including 475 methicillin-susceptible *S. aureus [*MSSA] and 513 MRSA) and 1053 *K. pneumoniae* isolates (including 536 carbapenem-susceptible *K. pneumoniae [*CSKP] and 517 CRKP) (Table 1). Of these, 626 *S. aureus* and 606 *K. pneumoniae* isolates were collected from the Surveillance of Multicentre Antimicrobial Resistance in Taiwan (SMART) program, which involved 16 regional hospitals across Taiwan between 2017 and 2020 [14,15]. The remaining 362 *S. aureus* and 447 *K. pneumoniae* isolates were obtained randomly from bacteraemia patients undergoing treatment from China Medical University Hospital (CMUH) between 2023 and 2024. Among these isolates, we randomly selected 200 *S. aureus* and 200 *K. pneumoniae* isolates from SMART, and 66 *S. aureus* and 85 *K. pneumoniae* isolates from CMUH for training, with the remaining isolates used for validation.

Bacterial isolates were cultured on blood agar plates (Tryticase soy agar [TSA] with 5% sheep blood, Becton–Dickinson Microbiology Systems, Sparks, MD, USA) at 37 °C for 16–18 h to facilitate colony formation. The identification of isolates was confirmed using MALDI-TOF and 16S rRNA sequencing. Antimicrobial susceptibility testing was subsequently performed using the automated Phoenix system (BD Phoenix M50, Becton–Dickinson Microbiology Systems, Sparks, MD, USA) to generate antibiotic susceptibility reports. The mechanisms underlying MRSA and CRKP were determined as previously described [14,15].

2.3. Preparation of Raman samples

Bacterial isolates were directly mixed with silver nanoparticles and excited using a 785 nm laser [16,17]. The representative Raman fingerprinting spectra of the bacteria were obtained by positioning the bacterial cell near the plasmonic silver nanoparticles. In a typical experiment, clinical bacterial isolates were cultured on blood

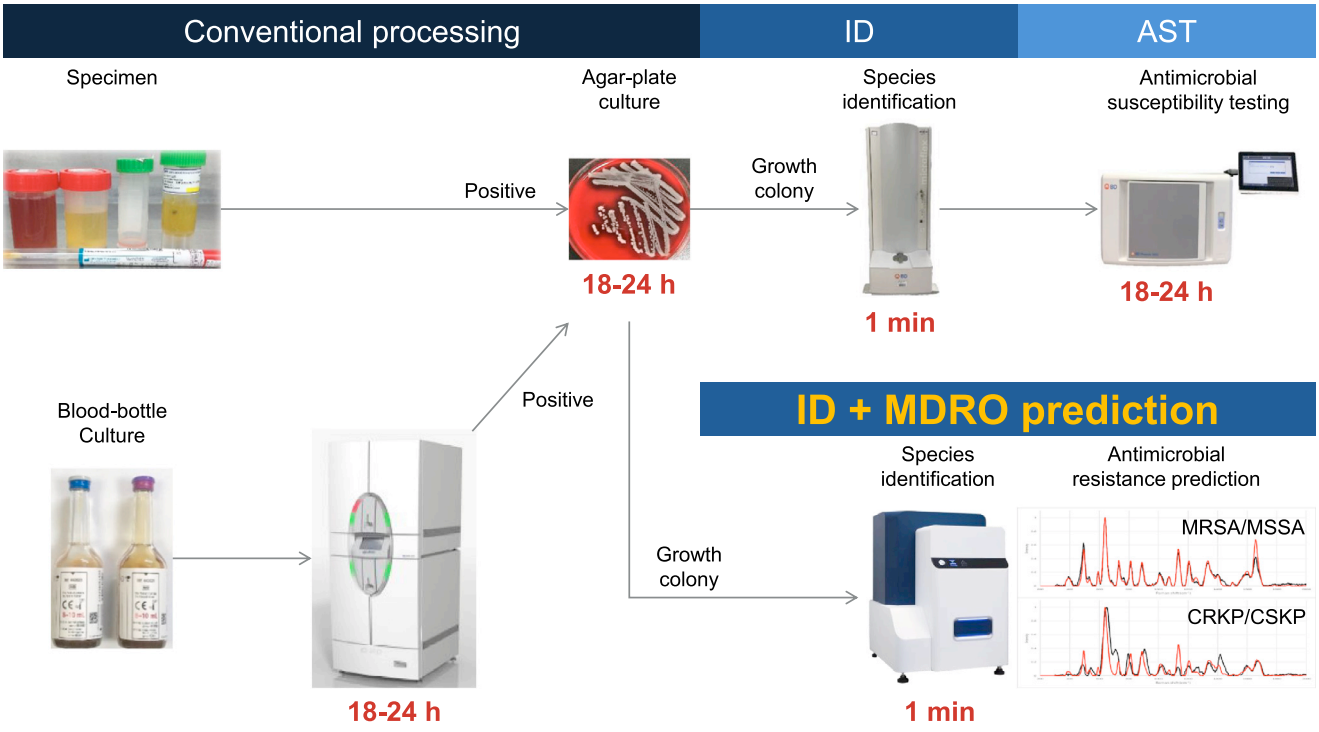

Fig. 1. Comparison of clinical workflows illustrating the time-saving benefits of using Raman spectroscopy combined with deep learning for predicting MDROs. The combined application of Raman spectroscopy and deep learning accelerates the clinical workflow for MDRO prediction. ID, identification; AST, antimicrobial susceptibility testing.

agar plates (TSA with 5% sheep blood, Becton–Dickinson Microbiology Systems, Sparks, MD, USA) at 37 °C for 16–18 h to enable colony formation. A single colony was then picked using a sterile inoculating loop and mixed with a silver nanoparticle SERS colloid (ITRUST MedTech Inc., Hsinchu, Taiwan) on a stainless-steel substrate (ITRUST MedTech Inc., Hsinchu, Taiwan). After rapid air-drying, a circle approximately 2 to 3 mm in diameter was formed.

2.4. Raman measurements

Raman scattering signals were measured using the AIRDIS system (ITRUST MedTech Inc., Hsinchu, Taiwan), with an integration time set to 1 s and laser power varying from 1 to 500 mW during the acquisition. To ensure the recognizability and consistency of Raman spectra, the AIRDIS system incorporates an acceptance threshold for minimum spectral intensity during the sampling process. Since laser power directly influences Raman signal intensity, the system dynamically adjusts the laser power in real-time during acquisition to meet this threshold. The AIRDIS system consists of a compact Raman spectrometer integrated with embedded machine learning modules for automated bacterial classification. It operates with dedicated components including proprietary detection substrates, reagents, and a calibration chip for system standardization. A connected computer with pre-installed AIRDIS software manages spectral acquisition, preprocessing, and resistance phenotype prediction. To account for the coffee-ring effect of the SERS colloid, the ring-shaped area was chosen as the optimal measurement position [18]. Spectra collected from 20 randomly selected points within the ring region exhibited high reproducibility.

2.5. Spectrum pretreatment

To ensure spectral consistency and maintain a linear relationship between signal intensity, irradiating laser power, and integration time, the spectra underwent baseline correction and smoothing. A polynomial fitting algorithm was employed for baseline correction, while the Savitzky-Golay filter was utilized for smoothing to preserve spectral features while reducing noise [19]. Subsequently, the spectra were normalized to standardize all features within the same range, enhancing comparability across different variables.

2.6. Data labelling process

Using the AIRDIS system, Raman spectra of microbial strains were collected. Simultaneously, the antibiotic susceptibility of these strains was determined using the automated Phoenix system. The antibiotic susceptibility results generated by automated Phoenix system were then matched with the corresponding Raman spectral data. For each sample, if it was classified as antibiotic-resistant (e.g., MRSA, CRKP), its corresponding Raman spectrum was labelled as 'resistant'. Conversely, if the strain was susceptible to antibiotics (e.g., MSSA, CSKP), it was labelled as 'susceptible'. These labelled data were subsequently used to train a deep learning model aimed at distinguishing between resistant and susceptible samples.

2.7. Deep learning model architecture and model training

Deep learning has been widely applied to classification tasks in different fields, including computer vision, fraud detection and medical diagnosis. Due to the data structure and Raman scattering properties of Raman spectrum, we adapted the RamanNet architecture for the antimicrobial resistance classification task [20]. First, the input Raman spectrum was divided into multiple overlapping fragments (fragment length = 100, overlapping length = 50). Second, each fragment was processed by a separate convolutional block consisting of a dense layer with 512 neurons, followed by batch normalization to extract features. The features from all fragments were then concatenated and regularized using a dropout

Table 2
Model hyperparameters used for antimicrobial resistance classification based on Raman spectra.

Hyperparameters	Value
Fragment length	100
Overlapping length	50
MLP neurons	512
Dropout	0.5
Optimizer	Adam
Learning rate	0.001
Loss function	Binary cross entropy loss
Training epochs	150

layer (dropout rate = 0.5). Finally, a multi-layer perceptron (MLP) was constructed for the task, consisting of two dense layers followed by batch normalization and an output layer.

The hyperparameters of the antimicrobial resistance classification models were tuned by a grid search on the training dataset. During training, the dataset was randomly split into an 8:2 ratio for training and validation. The weighted F1-score on the validation data was used for model selection. The final model was optimized using the Adam optimizer (learning rate = 0.001) and binary cross-entropy loss for 150 training epochs. The models were trained and evaluated using TensorFlow (version: 2.9.1), Keras (version: 2.9.0) and scikit-learn (version: 1.3.2) on a computer with Intel Core i7-14700 K CPU, 128 GB RAM and NVIDIA GeForce RTX 4090 GPU [21–23]. Model hyperparameters are summarized in Table 2.

To assess the performance of our model, we also implemented two traditional machine learning models, namely support vector machine (SVM) and random forest (RF), for comparison. Both machine learning models were trained and tuned using the same dataset employed for training the RamanNet model. The hyperparameters of the machine learning models were tuned by a grid search on the training dataset. Model hyperparameters of the machine learning models are summarized in Table S1.

2.8. SHAP value analysis for feature importance

To evaluate the significant Raman spectral features that influence the deep learning model's predictions, SHapley Additive exPlanations (SHAP) analysis (version: 0.44.1) was conducted [24]. SHAP values, representing the contribution of individual input features to the model's predictions, were calculated for each input. The mean absolute SHAP values were then mapped to their corresponding Raman shift positions to visualize the overall importance of Raman spectral features in antimicrobial resistance classification task.

2.9. Clinical identification data analysis

Each sample in the testing dataset included 20 Raman spectra. During model evaluation, the antimicrobial resistance score of each sample was calculated as the average score of the 20 Raman spectra predicted by the optimized model. A threshold of 0.5 was set to classify samples as resistant or susceptible. Model performance was assessed using metrics such as accuracy, AUROC, AUPRC, and F1 score, all calculated from the confusion matrix (data not shown). This matrix summarizes the model's performance by comparing predicted outcomes with actual results.

A confusion matrix is a useful tool for evaluating the performance of a classification model, as it displays the true positive, true negative, false positive, and false negative results for each class. The matrix allows for the calculation of various performance metrics, such as recall (sensitivity) and the precision, providing a comprehensive analysis of the model's ability to distinguish between different MDROs. Additionally, metrics like AUROC and AUPRC offer further insights into model performance. AUROC measures the model's ability to discriminate between classes across various threshold settings, providing a single value that reflects overall performance. In contrast, AUPRC emphasizes the balance between precision and recall at different thresholds, making it particularly useful for scenarios with imbalanced class distributions.

3. Results

3.1. Raman spectrum dataset for deep learning

To construct an antimicrobial resistance dataset for *S. aureus* and *K. pneumoniae* to support the development of deep learning models, we collected 988 isolates of *S. aureus* and 1053 isolates of *K. pneumoniae* from clinical samples. The species of isolates were confirmed using MALDI-TOF MS and 16S sequencing. MRSA isolates and CRKP isolates were detected by the automated Phoenix system (Becton–Dickinson Microbiology Systems, Sparks, MD, USA). After acquiring the Raman spectra, data pretreatment was performed using the AIRDIS system software (ITRUST MedTech Inc., Hsinchu, Taiwan) to ensure data consistency. Each bacterial sample in the dataset was measured for a minimum of 20 spectra (Fig. 2).

3.2. Identification of antibiotic resistance of *S. aureus* and *K. pneumoniae*

Two binary classification deep learning models were developed to identify antimicrobial resistance in *S. aureus* and *K. pneumoniae* using Raman spectroscopy. The *S. aureus* model (SA model) differentiated between MRSA and MSSA, while the *K. pneumoniae* model (KP model) distinguished between CRKP and CSKP (Table1). Among the 988 *S. aureus* isolates (containing 19 760 AIRDIS Raman spectrum files [RS files]) and 1053 *K. pneumoniae* isolates (containing 21 060 AIRDIS RS files), 266 *S. aureus* isolates (5320 AIRDIS RS files) and 285 *K. pneumoniae* isolates (5700 AIRDIS RS files) were selected for model training after spectral preprocessing to ensure data comparability. The remaining isolates were used as the test dataset (Table 3).

In the SA model, we developed a deep learning classification model to distinguish between MRSA and MSSA, achieving an overall accuracy of 88% (Table 3 and Fig. 3A). Misdiagnosing MRSA as MSSA can leads to more serious consequences than the reverse, so we adjusted the binary decision threshold to enhance sensitivity, thereby reducing the false-negative rate. The area under the receiver operating characteristic curve (AUROC) was 0.92, indicating that a randomly chosen positive sample (e.g., a Raman spectrum from an MRSA clinical isolate) is 92% more likely to be correctly predicted as MRSA compared to a randomly chosen negative sample (e.g., one from an MSSA clinical isolate) (Table 3 and Fig. 3B). For the KP model, we developed another deep learning classification model to differentiate between CRKP and CSKP, achieving an overall accuracy of 87% (Table 3 and Fig. 3C). The negative clinical impact of misclassifying CRKP as CSKP is no less significant than in the case of MRSA, so similar adjustments to the binary decision process were applied. The AUROC of 0.96 for this model indicates that a randomly selected positive sample – a Raman spectrum from clinical isolates with CRKP – is predicted as CRKP over a randomly selected negative sample – a Raman spectrum from clinical isolates with CSKP – with a probability of 0.96 (Table 3 and Fig. 3D).

Evaluation of the trained model showed high performance in predicting MRSA/MSSA and CRKP/CSKP, with metrics such as accuracy, AUROC, area under precision recall curve (AUPRC), and F1

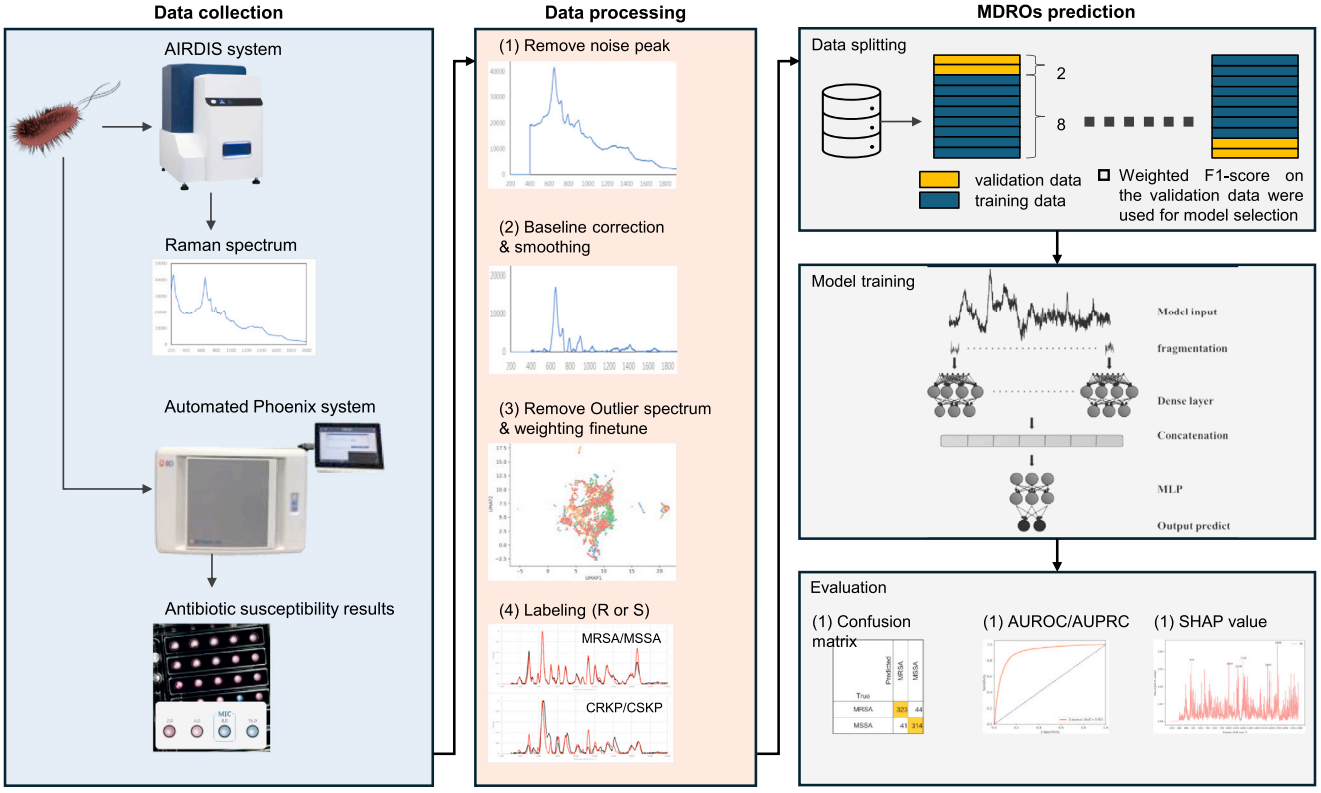

Fig. 2. Workflow for training a deep learning model to predict MDROs using Raman spectroscopy. Clinical isolates were collected, and Raman spectrum were acquired with the AIRDIS system. Antibiotic susceptibility profiles were obtained via the Phoenix system and matched with the Raman spectra. This labelled dataset was then used to train a deep learning model, allowing for the prediction of MDROs based on Raman spectrum.

Table 3
Model performances of predictions for methicillin-resistant *S. aureus* and carbapenem-resistant *K. pneumoniae*.

MDROs[a] (no. of isolates)	Accuracy	AUROC	AUPRC	Very major errors	Major errors	Recall	Precision	F1	MCC
S. aureus (988)[b]									
RamanNet	0.88	0.92	0.91	0.12	0.12	0.88	0.89	0.88	0.76
RF	0.75	0.84	0.85	0.15	0.34	0.85	0.72	0.78	0.51
SVM	0.75	0.83	0.83	0.16	0.34	0.84	0.72	0.77	0.50
K. pneumoniae (1053)[c]									
RamanNet	0.87	0.96	0.92	0.16	0.11	0.84	0.89	0.86	0.73
RF	0.70	0.76	0.74	0.28	0.33	0.72	0.69	0.70	0.40
SVM	0.67	0.74	0.73	0.28	0.37	0.72	0.66	0.69	0.35

[a] MDROs, Multidrug-resistant organisms; RS files, Raman spectrum files; AUROC, area under receiver operating characteristic; AUPRC, area under precision recall curve; MCC, Matthews Correlation Coefficient; RF, Random Forest; SVM, Support Vector Machine.
[b] The training and testing datasets consisted of 266 isolates (5320 Raman spectra) and 722 isolates (14440 Raman spectra), respectively.
[c] The training and testing datasets consisted of 285 isolates (5700 Raman spectra) and 768 isolates (15360 Raman spectra), respectively.

score indicating strong results (Table 3). Adjusting to a lower classification threshold can increase sensitivity of the model, reducing the risk of misclassifying resistant sample as susceptible. These results demonstrate the high predictive capability of the deep learning classification models, particularly in scenarios involving random sample selection.

To benchmark the performance of the classification models, we also evaluated two traditional machine learning algorithms, namely SVM and RF, using the same training and validation datasets. As shown in Table 3 and Fig. S1, both alternative models yielded lower AUROC values in both the SA and KP classification tasks, indicating that the deep learning models outperformed conventional approaches in distinguishing antimicrobial-resistant from susceptible isolates. Other performance metrics showed a similar trend. These findings further support the use of tailored deep learning architectures for Raman-based bacterial resistance profiling.

3.3. Raman spectra between antibiotic-resistant and antibiotic-susceptible isolates

The Raman spectra of MRSA and MSSA were compared, revealing high reproducibility due to their shared *S. aureus* characteristics (Fig. 4A). However, closer examination in a magnified view uncovers subtle differences in certain peak positions. Similarly, a comparison of the Raman spectra of CRKP and CSKP showed a similar trend (Fig. 4B). Additionally, SHAP (SHapley Additive exPlanations) analysis, an explainable AI (XAI) method based on game theoretic approach to calculate the cumulative contribution of individual features to model predictions, was applied to the models. The SHAP analysis result in Fig. 5 presents the top 20 most important Raman shift features, ranking by the mean absolute SHAP value. As shown in Fig. 5A, Raman shift features within the spectrum regions of 1688–1702 cm^{-1}, 1200–1227 cm^{-1}, 457–476 cm^{-1}, 1004 cm^{-1}, 1547–1606 cm^{-1} and 1128 cm^{-1} are identified as the

A

True \ Predicted	MRSA	MSSA
MRSA	323	44
MSSA	41	314

B

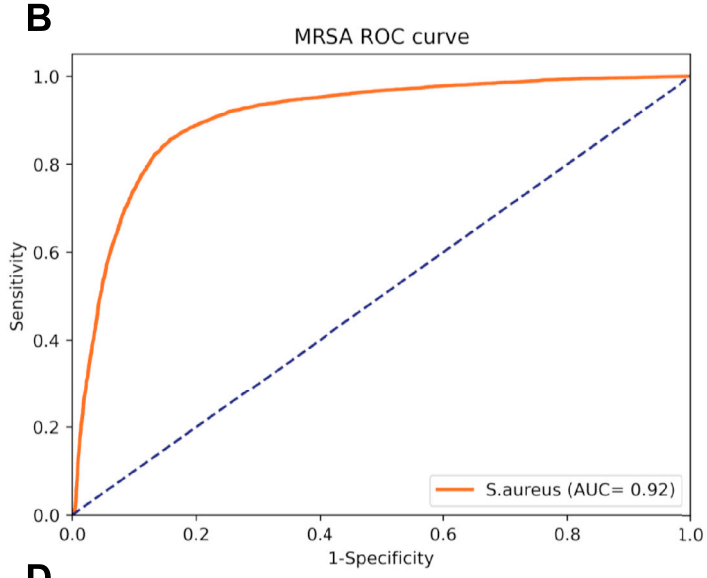

C

True \ Predicted	CRKP	CSKP
CRKP	324	61
CSKP	42	341

D

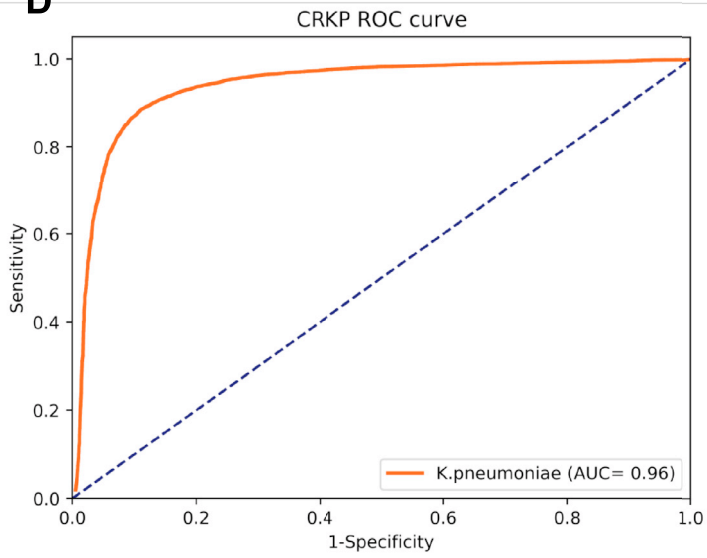

Fig. 3. Deep learning classification models for MRSA/MSSA and CRKP/CSKP differentiation. (**A**) The deep learning classification model was developed to distinguish between MRSA and MSSA, achieving 88% accuracy. (**B**) By varying the classification threshold, it is possible to trade-off between sensitivity (true positive rate) and specificity (true negative rate). The ROC curve shows sensitivities and specificities significantly higher than random classification, with an AUROC of 0.92. (**C**) The model to distinguish between CRKP and CSKP achieved an accuracy of 87%. (**D**) By varying the classification threshold, it is possible to trade-off between sensitivity (true positive rate) and specificity (true negative rate). The ROC curve shows sensitivities and specificities significantly higher than random classification, with an AUROC of 0.96.

most contributed features to the SA model's predictions. Similarly, Fig. 5B shows Raman shift features within the regions of 1654–1690 cm^{-1}, 1205 cm^{-1}, 1124–1133 cm^{-1}, 1438–1449 cm^{-1}, 1573–1577 cm^{-1}, 1267 cm^{-1} and 810–811 cm^{-1} are the most important features for the KP model.

To further investigate the relationship between the significant features and the underlying spectral differences within specific Raman shift regions, the mean absolute SHAP values of these features were mapped to their corresponding Raman shift positions (Fig. 4C and D). These values were then compared with Raman spectra of MRSA/MSSA and CRKP/CSKP (Fig. 4A and B) to analyse the spectral variations. In the SA model, distinct patterns observed at Raman shifts of 1004 cm^{-1} and 1547 cm^{-1}, along with slightly elevated peak intensities at shifts around 1128 cm^{-1}, 1200 cm^{-1} and 1688 cm^{-1}, were identified as key features for distinguishing MRSA from MSSA (Fig. 4C and Fig. 5A). In the KP model, spectral patterns within Raman shift range of 1125–1690 cm^{-1} and higher intensity around the 811 cm^{-1} shift were influential in differentiating CRKP from CSKP (Fig. 4D and Fig. 5B). These spectral differences, primarily related to variations in the relative intensities between adjacent peaks, confirm that antibiotic-resistant strains exhibit distinct Raman shift and scattering intensity behaviours. Such differences can be recognized by deep learning models for effective antimicrobial resistance identification.

4. Discussion

In our previous study, we successfully identified clinical isolates of *S. aureus, Enterococcus faecium, K. pneumoniae, Pseudomonas aeruginosa*, and *Acinetobacter baumannii* at the species level with high accuracy (94.76–96.88%) and an AUROC of 0.99 for all species [25]. In this study, we further implement deep learning technology to process the large amount of data obtained from Raman spectroscopy, enabling successfully differentiation between MRSA/MSSA and CRKP/CSSP. Due to the clinical significance of MRSA and CRKP infections and the increased mortality associated with delayed treatment [26], several commercial diagnostic methods have been developed to overcome the limitations of tradi-

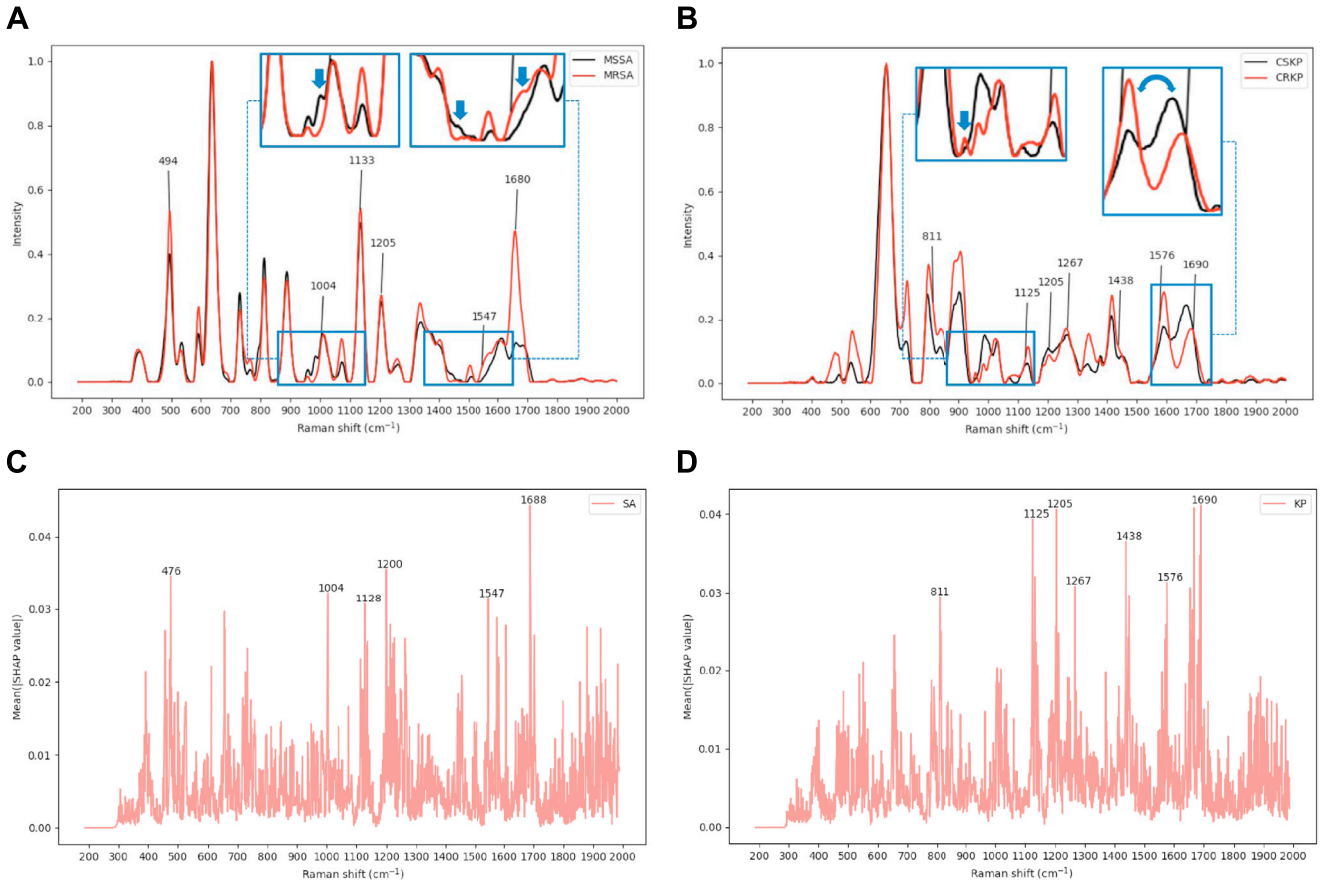

Fig. 4. Raman spectra and SHAP analysis of MRSA/MSSA and CRKP/CSKP. (**A**) The Raman spectra of *S. aureus* are shown, with the red line representing antibiotic-resistant isolates (MRSA) and the black line representing non-resistant isolates (MSSA). (**B**) The Raman spectra of *K. pneumoniae* are illustrated, with the red line indicating antibiotic-resistant isolates (CRKP) and the black line indicating non-resistant isolates (CSKP). (**C**) For SA model, the mean absolute SHAP values of the input features are mapped to their corresponding Raman shift positions, with Raman shift regions showing SHAP values higher than 0.03 highlighted. (**D**) For KP model, the mean absolute SHAP values of the input features are similarly mapped to their corresponding Raman shift positions, highlighting Raman shift regions with SHAP values exceeding 0.03. The arrows indicate spectral differences in the pattern or relative intensity of these Raman shift ranges.

tional workflows. Common approaches include PCR-based assays for resistance gene detection and immunodetection methods for resistance-related proteins. While these technologies are useful, most require additional instruments or manual steps, which increase the workload of laboratory personnel and overall healthcare costs [27]. The AIRDIS equipment used in this study was specifically developed to meet clinical demands, addressing the high volume of diagnostic tests in clinical settings. A simplified sample preparation process was devised to support batch operations, with specialized detection substrates enabling the analysis of up to 96 samples in a single run. The AIRDIS also facilitates fully automated measurements, with each sample taking only 1–3 minutes for complete analysis. While the system shows promising performance, its current application is limited to specific resistance phenotypes and still requires further clinical validation before widespread use.

Previous studies have demonstrated the potential of Raman spectroscopy in microbial detection [28]. However, its clinical application remains limited due to technical challenges such as strong fluorescence background and spectral variability [29]. Previous studies have shown that Surface-enhanced Raman scattering (SERS) spectra outperform normal Raman spectra in bacterial detection [30]. In our study, we addressed these limitations by adopting standardized detection substrates and an automated sampling strategy based on SERS. Furthermore, the high similarity of Raman spectra between different bacterial species, as well as between resistant and susceptible strains of the same species [31–34]. Using manual or simple mathematical models to compare characteristic peaks and analyse differences between datasets is time-consuming and lacks sufficient discriminatory power. Therefore, we sought to use machine learning (ML) and artificial intelligence (AI) to identify these numerous, subtle, hard-to-detect spectral features. In addition, there are concerns regarding the reproducibility and repeatability of SERS [35]. To minimize signal inconsistency, we collected spectra from 20 randomly selected points per sample and used automated image recognition to identify optimal sampling areas.

Previous studies using Raman spectroscopy to differentiate MRSA and MSSA reported accuracies of 89% and 100%, while accuracies of 99.87% and 100% were achieved for distinguishing CRKP and CSKP [8,10,11]. In our study, the accuracy for distinguishing MRSA and MSSA was 88%, and for distinguishing CRKP from CSKP, it was 87%. However, previous studies were primarily small-scale and involved fewer or standard strains, whereas our study included 988 *S. aureus* and 1053 *K. pneumoniae* isolates, all of which were clinical isolates. Despite significantly increasing the number of isolates and using clinical isolates, we achieved satisfactory accuracy levels. This validates the potential of the Raman spectroscopy combined with a machine learning approach for direct application in detecting resistant isolates in clinical microbiology laboratory.

Previous studies using a 785 nm excitation source to compare Raman spectra between MRSA and MSSA have identified carotenoid-related peaks at 1523 cm^{-1}, 1160 cm^{-1}, and 1007 cm^{-1}, likely corresponding to staphyloxanthin, a pigment found in *S. au-*

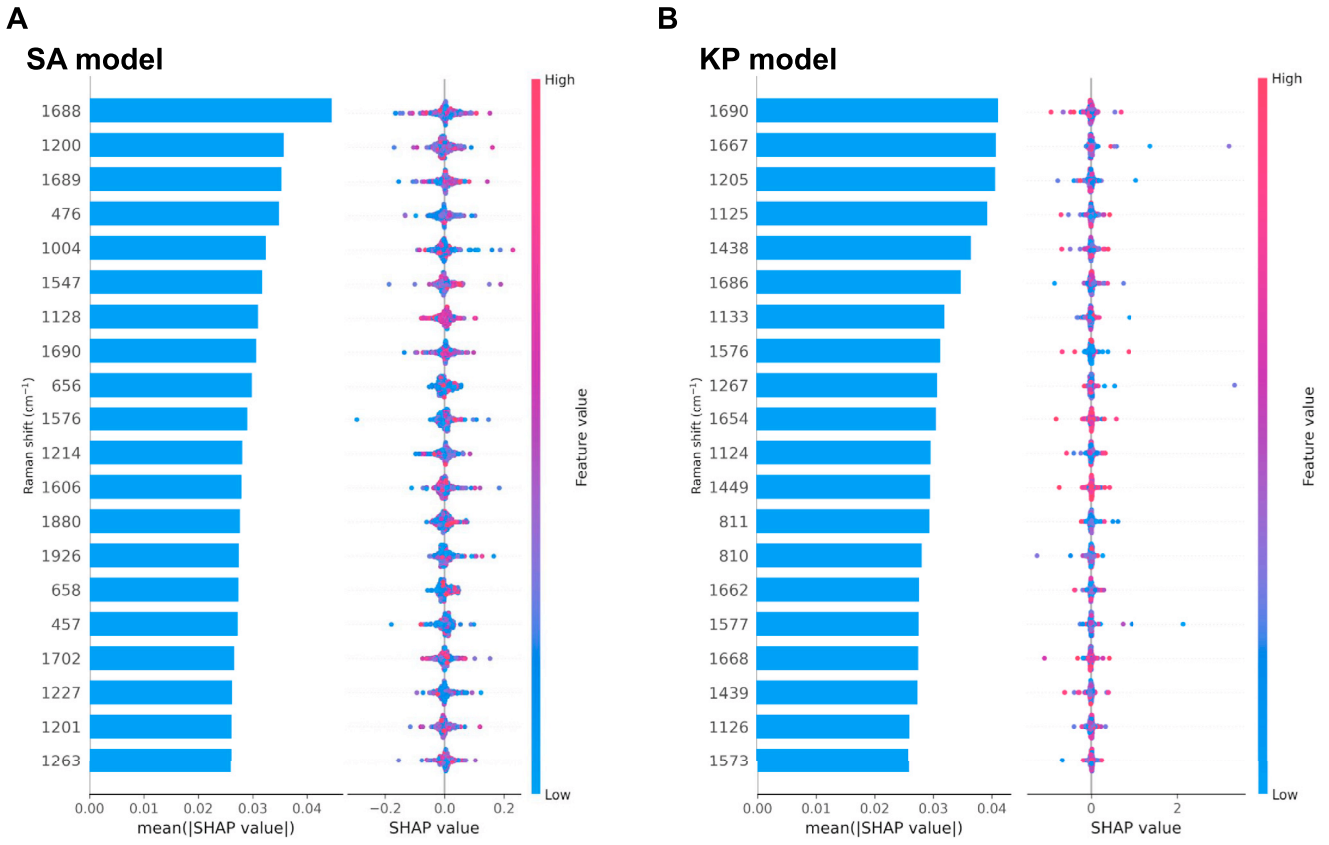

Fig. 5. Identification of important Raman spectrum feature on *S. aureus* (SA) and *K. pneumoniae* (KP) models using SHapley Additive exPlanations (SHAP) Analysis. The SA model differentiated between methicillin-resistant *S. aureus* and methicillin-susceptible *S. aureus*, while the KP model distinguished between carbapenem-resistant *K. pneumoniae* and carbapenem-susceptible *K. pneumoniae*. (A) and (B) display the SHAP analysis result for the SA and KP models, using a bar plot on the left panel and a dot plot on the right panel. The bar plot presents the mean absolute SHAP value, representing the average contribution of each feature to model's predictions, specifically for the top 20 most important Raman shift features. The dot plot shows the distribution of SHAP values across all test samples, illustrating the variability in each feature's impact on model's predictions. The colour of each dot represents the intensity of each feature within the test samples, showing the correlation between low and high intensity and their associated impact on the model's predictions.

reus [36]. Similar spectral differences were observed at nearby shifts in this study. Although staphyloxanthin is more strongly associated with virulence than resistance, these spectral variations suggest potential biochemical differences between MRSA and MSSA that may contribute to the classification performance of the SA model. In the KP model, Raman shifts at 1654–1690 cm^{-1}, 1205 cm^{-1}, 1124–1133 cm^{-1}, 1438–1449 cm^{-1}, 1573–1577 cm^{-1}, 1267 cm^{-1}, and 810–811 cm^{-1} were found to differ between CRKP and CSKP. Previous studies using 785 nm excitation have shown that peaks at 1180 cm^{-1}, 1445 cm^{-1}, and 1688 cm^{-1} are associated with C–O–C and =C–C= antisymmetric stretching in aliphatic esters and glycosidic linkages of carbohydrates, CH_2 vibrations of membrane lipids and polysaccharides, and the amide I band of proteins and lipids, respectively. These features may originate from lipopolysaccharide (LPS). Although LPS is not a direct cause of carbapenem resistance, structural changes in LPS may reduce antibiotic binding affinity [13,37].

The deep learning-based Raman spectroscopy approach enables faster detection and prediction of various multidrug-resistant organisms (MDROs), such as MRSA and CRKP. Since this approach bypasses conventional culture-based AST, it can provide results within minutes following species identification. This may allow for earlier alerts than traditional AST and assist clinicians in making more timely and informed antibiotic decisions. Additionally, by reducing the risk of antibiotic misuse, this method supports global public health efforts.

Our team previously developed the Intelligent Antimicrobial System (iAMS), which combined MALDI-TOF MS spectra with machine learning for predicting MRSA and CRKP, and achieved favourable clinical outcomes in a hospital setting [38,39]. Based on the experience, we designed the AIRDIS system to offer similar predictive capabilities using Raman spectroscopy, but in a more accessible format. Unlike MALDI-TOF MS, which requires expensive instrumentation and centralized computational infrastructure, AIRDIS is compact, includes built-in AI processing, and is more affordable in terms of both initial and ongoing costs. Current AI-integrated Raman systems are limited in scope, often lacking either resistance prediction or species identification capabilities [8,40]. In contrast, AIRDIS provides both, and was validated using a large number of clinical isolates. It supports batch processing, automated measurement, and rapid analysis, and can be incorporated into existing clinical workflows without the need for additional equipment or significant operational overhead. Its relatively low operational cost makes it particularly suitable for smaller hospitals and resource-limited settings. The model architecture is modular, allowing for future expansion to include additional pathogens and resistance phenotypes, further enhancing its potential clinical utility.

There were some limitations in the present study. First, the prediction was only performed for MRSA and CRKP and did not include the detection of specific AMR genotypes. Therefore, the current system cannot fully replace conventional AST methods.

Second, although we identified certain Raman shifts that differed between resistant and susceptible isolates and proposed possible molecular components based on literature, whether these components can serve as reliable biomarkers for resistance still requires further investigation. Third, although the resistance genes and resistance profiles of many isolates are known, we were unable to determine whether they affected prediction outcomes or contributed to misclassifications. Moreover, while the system can identify CRKP, it is currently unable to distinguish between different resistance mechanisms such as KPC, NDM, or OXA-48. This limitation reduces its ability to guide the selection of newer antibiotics. Further studies with a larger and more diverse set of isolates will be necessary to address this limitation and expand the model's capability to detect a broader range of resistance phenotypes. Further investigation is warranted. Finally, additional validation using a larger number of clinical isolates will be necessary before clinical implementation of the system.

5. Conclusions

In conclusion, we developed a bacterial identification system, AIRDIS, which combines Raman spectroscopy with machine learning to perform species identification and predict resistant strains, including MRSA and CRKP. The system is fast and cost-effective, making it suitable for small to medium-sized hospitals.

Declarations

Funding: This study was supported by the grant NSTC 113-2320-B-039-010 from the National Science and Technology Council of Taiwan and CMU113-MF-67 from China Medical University, Taichung, Taiwan.

Declaration of competing interests: None declared.

Ethical approval: Not required.

Data availability: The data supporting the findings of this study are not publicly available due to proprietary restrictions and ongoing patent protection but may be available from the corresponding author upon reasonable request and subject to applicable intellectual property agreements.

Author contributions: All authors were involved in the conception, design, and funding application for the study. HHL, YTL, KHT, and PCH conducted all bacterial sample experiments. CHC and YLW developed the integration of the predictive system with the hospital reporting system. NSL, YFC, CYH, and YHL performed all machine learning analysis experiments. All authors were involved in the interpretation of the outputs. YTL, NSL, and CYH wrote the manuscript with the assistance and feedback of all co-authors. PRH and DYC conceived and supervised the study. All authors have read and approved the manuscript.

Acknowledgements: Investigators from the SMART program 2017–2020: Wen-Sen Lee (Wan Fang Hospital, Taipei), Min-Chi Lu (China Medical University Hospital, Taichung), Zhi-Yuan Shi (Taichung Veterans General Hospital, Taichung), Yao-Shen Chen (Kaohsiung Veterans General Hospital, Kaohsiung), Lih-Shinn Wang (Buddhist Tzu Chi General Hospital, Hualien), Shu-Hui Tseng (Ministry of Health and Welfare, Taipei), Chao-Nan Lin (National Pingtung University of Science and Technology, Pingtung), Yin-Ching Chuang (Chi Mei Hospital, Tainan), Yu-Hui Chen (Chi Mei Hospital, Tainan), Wang-Huei Sheng (National Taiwan University Hospital, Taipei), Chang-Pan Liu (MacKay Memorial Hospital, Taipei), Ting-Shu Wu (Chang Gung Memorial Hospital, Taoyuan), Chun-Ming Lee (St Joseph's Hospital, Yunlin), Po-Liang Lu (Kaohsiung Medical University Hospital, Kaohsiung), Muh-Yong Yen (Taipei City Hospital, Taipei), Pei-Lan Shao (National Taiwan University Hospital, Hsin-Chu), Shu-Hsing Cheng (Taoyuan General Hospital, Taoyuan), Chi-Ying Lin (National Taiwan University Hospital, Yun-Lin), Ming-Huei Liao (National Pingtung University of Science and Technology, Pingtung), Yen-Hsu Chen (Kaohsiung Medical University, Kaohsiung), Wen-Chien Ko (National Cheng Kung University Hospital, Tainan), Fu-Der Wang (Taipei Veterans General Hospital, Taipei) and Po-Ren Hsueh (China Medical University Hospital, Taichung. Taiwan).

Supplementary materials

Supplementary material associated with this article can be found, in the online version, at doi:10.1016/j.ijantimicag.2025.107587.

References

[1] Jesudason T. WHO publishes updated list of bacterial priority pathogens. Lancet Microbe 2024;5:100940.
[2] Yu J, Tien N, Liu Y-C, Cho D-Y, Chen J-W, Tsai Y-T, et al. Rapid identification of methicillin-resistant *Staphylococcus aureus* using MALDI-TOF MS and machine learning from over 20,000 clinical isolates. Microbiol Spectr 2022;10:e0048322.
[3] Seymour CW, Gesten F, Prescott HC, Friedrich ME, Iwashyna TJ, Phillips GS, et al. Time to treatment and mortality during mandated emergency care for sepsis. N Engl J Med 2017;376:2235–44.
[4] Tang J-W, Yuan Q, Zhang L, Marshall BJ, Yen Tay AC, Wang L. Application of machine learning-assisted surface-enhanced Raman spectroscopy in medical laboratories: principles, opportunities, and challenges. TrAC Trends Anal Chem 2025;184:118135.
[5] Butler HJ, Ashton L, Bird B, Cinque G, Curtis K, Dorney J, et al. Using Raman spectroscopy to characterize biological materials. Nat Protoc 2016;11:664–87.
[6] Lorenz B, Wichmann C, Stockel S, Rosch P, Popp J. Cultivation-free raman spectroscopic investigations of bacteria. Trends Microbiol 2017;25:413–24.
[7] Tang JW, Yuan Q, Wen XR, Usman M, Tay ACY, Wang L. Label-free surface-enhanced Raman spectroscopy coupled with machine learning algorithms in pathogenic microbial identification: current trends, challenges, and perspectives. Interdiscip Med 2024;2:e20230060.
[8] Ho CS, Jean N, Hogan CA, Blackmon L, Jeffrey SS, Holodniy M, et al. Rapid identification of pathogenic bacteria using Raman spectroscopy and deep learning. Nat Commun 2019;10:4927.
[9] Alzubaidi L, Zhang J, Humaidi AJ, Al-Dujaili A, Duan Y, Al-Shamma O, et al. Review of deep learning: concepts, CNN architectures, challenges, applications, future directions. J Big Data 2021;8:53.
[10] Liu W, Tang JW, Lyu JW, Wang JJ, Pan YC, Shi XY, et al. Discrimination between carbapenem-resistant and carbapenem-sensitive *Klebsiella pneumoniae* strains through computational analysis of surface-enhanced Raman spectra: a pilot study. Microbiol Spectr 2022;10:e0240921.
[11] Guo G, Guo C, Qie X, He D, Meng S, Su L, et al. Correlation analysis between Raman spectral signature and transcriptomic features of carbapenem-resistant *Klebsiella pneumoniae*. Spectrochim Acta Mol Biomol Spectrosc 2024;308:123699.
[12] Lu J, Chen J, Liu C, Zeng Y, Sun Q, Li J, et al. Identification of antibiotic resistance and virulence-encoding factors in *Klebsiella pneumoniae* by Raman spectroscopy and deep learning. Microb Biotechnol 2022;15:1270–80.
[13] Lyu JW, Zhang XD, Tang JW, Zhao YH, Liu SL, Zhao Y, et al. Rapid prediction of multidrug-resistant *Klebsiella pneumoniae* through deep learning analysis of SERS spectra. Microbiol Spectr 2023;11:e0412622.
[14] Huang YT, Kuo YW, Lee NY, Tien N, Liao CH, Teng LJ, et al. Evaluating NG-Test CARBA 5 multiplex immunochromatographic and cepheid xpert CARBA-R assays among carbapenem-resistant *Enterobacterales* isolates associated with bloodstream infection. Microbiol Spectr 2022;10:e0172821.
[15] Chen CH, Wu PH, Lu MC, Ho MW, Hsueh PRGroup SPS. National surveillance of antimicrobial susceptibilities to ceftaroline, dalbavancin, telavancin, tedizolid, eravacycline, omadacycline, and other comparator antibiotics, and genetic characteristics of bacteremic *Staphylococcus aureus* isolates in adults: results from the Surveillance of Multicentre Antimicrobial Resistance in Taiwan (SMART) program in 2020. Int J Antimicrob Agents 2023;61:106745.
[16] Liu Y, Zhou H, Hu Z, Yu G, Yang D, Zhao J. Label and label-free based surface-enhanced raman scattering for pathogen bacteria detection: a review. Biosens Bioelectron 2017;94:131–40.
[17] Hunter R, Sohi AN, Khatoon Z, Berthiaume VR, Alarcon EI, Godin M, et al. Optofluidic label-free SERS platform for rapid bacteria detection in serum. Sens Actuators B Chem 2019;300:126907.
[18] Šimáková P, Kočišová E, Procházka M. Coffee ring" effect of Ag colloidal nanoparticles dried on glass: impact to surface-enhanced raman scattering (SERS). J Nanomater 2021;2021:4009352.

[19] Zimmermann B, Kohler A. Optimizing Savitzky-Golay parameters for improving spectral resolution and quantification in infrared spectroscopy. Appl Spectrosc 2013;67:892–902.
[20] Ibtehaz N, Chowdhury MEH, Khandakar A, Kiranyaz S, Rahman MS, Zughaier SM. RamanNet: a generalized neural network architecture for Raman spectrum analysis. Neural Comput Appl 2023;35:18719–35.
[21] Pang B, Nijkamp E, Wu YN. Deep learning with tensorflow: a review. J Educ Behav Stat 2020;45:227–48.
[22] Zollanvari A. Deep learning with Keras-TensorFlow. In: Zollanvari A, editor. Machine Learning with Python: Theory and Implementation. Cham: Springer International Publishing; 2023. p. 351–91.
[23] Raschka S, Liu YH, Mirjalili V. Machine Learning with PyTorch and Scikit-Learn: Develop machine learning and deep learning models with Python. Birmingham, UK: Packt Publishing Ltd; 2022.
[24] Lundberg SM, Lee S-I. A unified approach to interpreting model predictions. Adv Neural Inf Process Syst 2017;30:4765–74.
[25] Lin Y-T, Lin H-H, Chen C-H, Tseng K-H, Hsu P-C, Wu Y-L, et al. Identification of *Staphylococcus aureus, Enterococcus faecium, Klebsiella pneumoniae, Pseudomonas aeruginosa* and *Acinetobacter baumannii* from Raman spectra by Artificial Intelligent Raman Detection and Identification System (AIRDIS) with machine learning. J Microbiol Immunol Infect 2025;58:77–85.
[26] Lee YL, Chen HM, Hii IM, Hsueh PR. Carbapenemase-producing *Enterobacterales* infections: recent advances in diagnosis and treatment. Int J Antimicrob Agents 2022;59:106528.
[27] Yu J, Lin HH, Tseng KH, Lin YT, Chen WC, Tien N, et al. Prediction of methicillin-resistant *Staphylococcus aureus* and carbapenem-resistant *Klebsiella pneumoniae* from flagged blood cultures by combining rapid Sepsityper MALDI-TOF mass spectrometry with machine learning. Int J Antimicrob Agents 2023;62:106994.
[28] Rebrosova K, Siler M, Samek O, Ruzicka F, Bernatova S, Hola V, et al. Rapid identification of staphylococci by raman spectroscopy. Sci Rep 2017;7:14846.
[29] Wei D, Chen S, Liu Q. Review of fluorescence suppression techniques in raman spectroscopy. Appl Spectrosc Rev 2015;50:387–406.
[30] Witkowska E, Nicinski K, Korsak D, Szymborski T, Kaminska A. Sources of variability in SERS spectra of bacteria: comprehensive analysis of interactions between selected bacteria and plasmonic nanostructures. Anal Bioanal Chem 2019;411:2001–17.
[31] Sundaram J, Park B, Kwon Y, Lawrence KC. Surface enhanced Raman scattering (SERS) with biopolymer encapsulated silver nanosubstrates for rapid detection of foodborne pathogens. Int J Food Microbiol 2013;167:67–73.
[32] Yang D, Zhou H, Dina NE, Haisch C. Portable bacteria-capturing chip for direct surface-enhanced Raman scattering identification of urinary tract infection pathogens. R Soc Open Sci 2018;5:180955.
[33] Li J, Wang C, Kang H, Shao L, Hu L, Xiao R, et al. Label-free identification carbapenem-resistant *Escherichia coli* based on surface-enhanced resonance raman scattering. RSC Adv 2018;8:4761–5.
[34] Tien N, Lin TH, Hung ZC, Lin HS, Wang IK, Chen HC, et al. Diagnosis of bacterial pathogens in the urine of urinary-tract-infection patients using surface-enhanced Raman spectroscopy. Molecules 2018;23:3374.
[35] Xiong M, Ye J. Reproducibility in surface-enhanced Raman spectroscopy. J Shanghai Jiaotong Univ Sci 2014;19:681–90.
[36] Pistiki A, Monecke S, Shen H, Ryabchykov O, Bocklitz TW, Rosch P, et al. Comparison of different label-free Raman spectroscopy approaches for the discrimination of clinical MRSA and MSSA isolates. Microbiol Spectr 2022;10:e0076322.
[37] Pruss A, Kwiatkowski P, Lopusiewicz L, Masiuk H, Sobolewski P, Fijalkowski K, et al. Evaluation of chemical changes in laboratory-induced colistin-resistant *Klebsiella pneumoniae*. Int J Mol Sci 2021;22:7104.
[38] Ho LC, Yu Chi C, You YS, Hsieh YW, Hou YC, Lin TC, et al. Impact of the implementation of the Intelligent Antimicrobial System (iAMS) on clinical outcomes among patients with bacteraemia caused by methicillin-resistant *Staphylococcus aureus*. Int J Antimicrob Agents 2024;63:107142.
[39] Yu J, Lin YT, Chen WC, Tseng KH, Lin HH, Tien N, et al. Direct prediction of carbapenem-resistant, carbapenemase-producing, and colistin-resistant *Klebsiella pneumoniae* isolates from routine MALDI-TOF mass spectra using machine learning and outcome evaluation. Int J Antimicrob Agents 2023;61:106799.
[40] Yi X, Song Y, Xu X, Peng D, Wang J, Qie X, et al. Development of a fast Raman-assisted antibiotic susceptibility test (FRAST) for the antibiotic resistance analysis of clinical urine and blood samples. Anal Chem 2021;93:5098–106.